Rock Mech. Rock Engng. (2005) 38 (2), 153–167
DOI 10.1007/s00603-004-0043-2

**Rock Mechanics
and Rock Engineering**
Printed in Austria

Technical Note

Dynamic Displacement of a Block on an Inclined Plane: Analytical, Experimental and DDA Results

By

M. Tsesarsky[1], **Y. H. Hatzor**[1], and **N. Sitar**[2]

[1] Department of Geological and Environmental Sciences,
Ben Gurion University of the Negev, Beer–Sheva, Israel
[2] Department of Civil Engineering, University of California,
Berkeley, California, USA

Received July 3, 2003; accepted May 5, 2004
Published online February 9, 2005 © Springer-Verlag 2005

Keywords: DDA, shaking table, block on incline, numerical error.

1. Introduction

Existing methods for evaluating ground performance under seismic loading fall into three categories (Cai and Bathurst, 1995): 1) force based pseudo-static methods; 2) displacement based (Newmark) methods; 3) numerical methods (FEM, DEM).

Typically, earthquake damage is associated with finite displacements of large discrete masses. Therefore, slope performance should be evaluated in terms of permanent displacements rather than in terms of safety factor derived from pseudo-static analysis. This approach was firstly introduced by Goodman and Seed (1965) and by Newmark (1965), and is now largely referred to as ‘‘Newmark’’ type analysis.

A Newmark type analysis assumes that relative slope movement is initiated when inertial forces on the potential sliding mass overcome the shear resistance along the sliding plane, the corresponding level of horizontal acceleration known as ‘‘yield acceleration’’. The analysis assumes that the mass will come to rest when it attains zero velocity. The permanent displacement of the sliding mass can then be calculated by integrating the relative velocity of the block during sliding over time.

Most rock masses are discontinuous by nature, and the intersection of discontinuities typically yields a network of individual blocks. When subjected to a dynamic load the individual blocks interact by transferring normal and tangential forces at the contacts. The developed failure mode will manifest the geometrical constrains and the forces acting upon the block system.

Realistic deformation simulation of a large number of blocks using a discrete numerical approach, such as the distinct element method – DEM (Cundall, 1971) or the discontinuous deformation analysis – DDA (Shi, 1988; 1993), requires rigorous validation using analytical solutions, physical models, and case studies. In this paper we use the DDA method for dynamic analysis.

Yeung (1991), MacLaughlin (1997) and Doolin and Sitar (2002) tested the accuracy of DDA using analytical solutions for the block on an incline problem. Hatzor and Feintuch (2001) validated DDA using direct dynamic input, for the same problem. The conclusions of these studies was that DDA is capable of predicting block displacements with high accuracy provided that the numeric control parameters are properly conditioned. McBride and Scheele (2001) validated DDA using a physical model of a multi-block array on a stepped base subjected to gravitational loading, concluding that kinetic damping is required for reliable displacement prediction.

In this paper we study the displacement history of a single block on an incline subjected to dynamic loading. The following issues are addressed:

1. Comparison between DDA and analytical solutions.
2. Comparison between DDA solution and shaking table results.
3. The role and sensitivity of the numeric control parameters in DDA.
4. The computational error in DDA.

2. Experimental Setting

The physical modeling used in this research was performed by Wartman et al. (2003) at the Earthquake Simulation Laboratory of the University of California at Berkley. The tests were performed on a large hydraulic driven shaking table, producing accurate, well controlled, and repeatable motions to frequencies up to 14 Hz. The table was driven by an MTS closed loop servo controlled hydraulic actuator. A Hewlett Packard 33120A arbitrary function generator produced the table command signal.

A steel plane, inclined by 11.37°, was fitted to the shaking table. A steel block, 2.54 cm thick, with area of 25.8 cm^2, and weight of 1.6 kg was positioned on top of the inclined plane. Linear accelerometers were fitted on top of the sliding block and the inclined plane. Displacement transducers measured the relative displacement of the sliding block, and of the shaking table (Fig. 1). In this study eight sinusoidal input motion tests were used for validation. The input frequencies, amplitudes, and block displacements are given in Table 1.

A geotextile and a geomembrane were fitted to the face of the sliding block and the inclined plane respectively. The static friction angle (ϕ) of the interface was determined by Wartman using tilt tests and a value of $\phi = 12.7° \pm 0.7°$ was reported. Kim et al. (1999) found that the friction angle of the geotextile–geomembrane interface exhibited pronounced strain rate effects, and reported an increase by 20% over one log-cycle of strain rate. Wartman (1999) showed that the friction angle of the interface

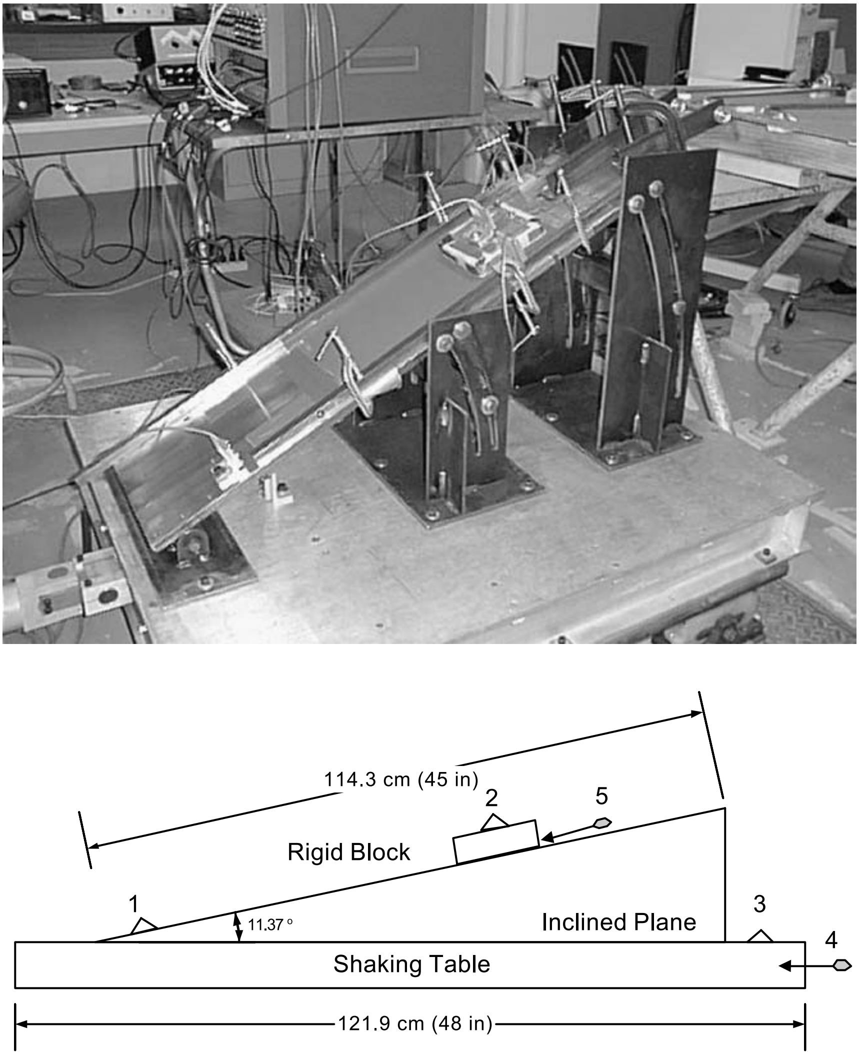

No.	Instrument	Direction of Measurement
1	accelerometer	parallel to plane
2	accelerometer	parallel to plane
3	accelerometer	horizontal
4	displacement transducer	horizontal
5	displacement transducer	parallel to plane

Fig. 1. a) General view of the inclined plane and the sliding block (top); **b**) Sliding block experimental setup and instrumentation location, from Wartman (1999)

was controlled by two factors: 1) amount of displacement; and 2) sliding velocity. The back-calculated friction angle for the range of velocities and displacements measured was in the range of $\phi = 14°–19°$ (Fig. 2).

Table 1. Shaking table model summary: ω is the input motion frequency, d_T is the shaking table displacement, d_B is relative block displacement, and a_h is maximum horizontal table acceleration

Test	ω (Hz)	d_T (cm)	d_B (cm)	a_h (g)
1	2.66	0.889	5.367	0.28
2	4	0.559	6.604	0.25
3	5.33	0.305	3.341	0.19
4	6	0.254	3.647	0.19
5	6.67	0.254	3.410	0.22
6	7.3	0.228	3.353	0.22
7	8	0.228	3.937	0.23
8	8.66	0.019	2.882	0.21

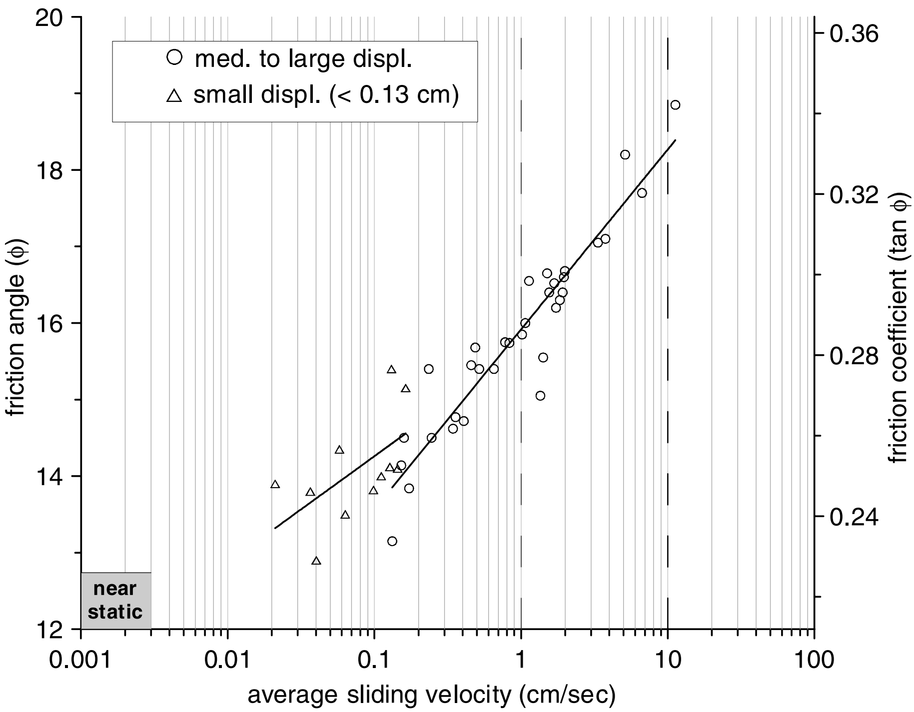

Fig. 2. Back calculated friction angles as a function of average sliding velocity for the rigid block tests, from Wartman (1999)

The DDA version used in this research accepts a constant value of friction angle. Therefore a single friction angle (ϕ_{av}) value must be chosen for validation. The value of ϕ_{av} was determined as follows. First, the measured displacement of the block was differentiated (forward difference) with respect to time and hence the velocity record was attained. The differentiation was performed for $\Delta t = 0.005$ sec, conforming to test acquisition rate of 200 Hz. Next, the velocity content for the duration of the test was computed. For an example, the 2.66 Hz input motion test showed that the upper a

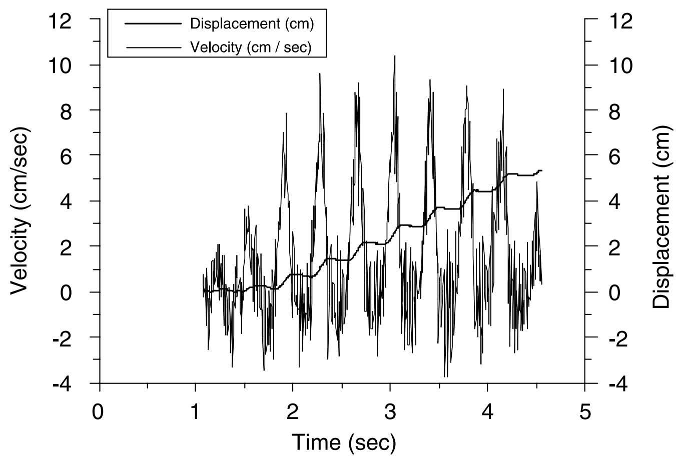

b

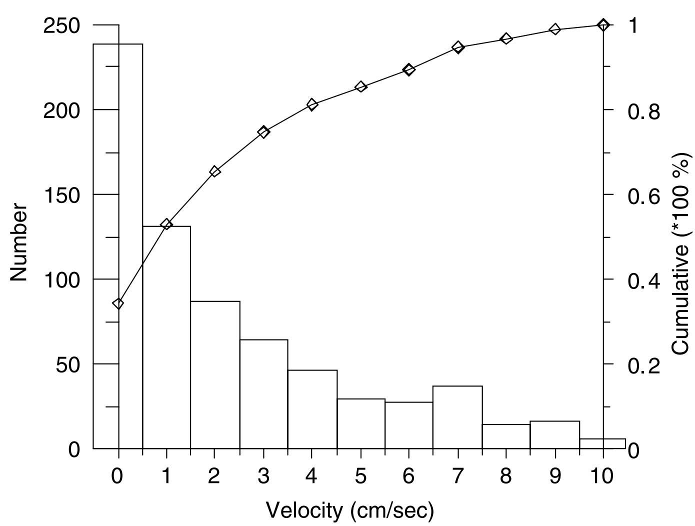

Fig. 3. **a**) Displacement derived velocity, 2.66 Hz sinusoidal input test; **b**) Velocity content of the 2.66 Hz sinusoidal input test

bound velocity value was below 10 cm/sec (Fig. 3a). This value was attained only for short periods during the test (Fig. 3b). The velocity content chart (Fig. 3b) shows that 80% of the velocities fall under 3 cm/sec (Fig. 3b). Taking 3 cm/sec as the upper bound velocity, the corresponding friction angle should be $\phi_{av} < 17°$ (Fig. 2). The 50% is 1 cm/sec value corresponding to friction angle of $\phi_{av} = 16°$. In all DDA simulations a constant value of $\phi_{av} = 16°$ was used for the validation study. It should be noted that velocity dependence is a test artifact associated with particular geo-interface used, and is not expected in rock discontinuities (e.g. Crawford and Curran, 1981).

3. DDA Formulation

DDA models a discontinuous material as a system of individually deformable blocks that move independently without interpenetration. In the DDA method the formulation of the blocks is very similar to the definition of a finite element mesh, where the elements are physically isolated blocks bounded by pre-existing discontinuities. The blocks used in DDA can assume any given geometry, as oppose to the predetermined topologies of the FEM elements.

By the second law of thermodynamics, a mechanical system under loading must move or deform in a direction that produces the minimum total energy of the whole system. For a block system the total energy consists of the kinetic energy, potential energy, strain energy and the dissipated energy. In DDA individual blocks form a system of blocks through contacts among blocks and displacement constrains on a single block. For a system of n blocks the simultaneous equilibrium equations, derived by minimizing the total energy Π of the block system are:

$$\begin{pmatrix} K_{11} & K_{12} & K_{13} & \cdots & K_{1n} \\ K_{21} & K_{22} & K_{23} & \cdots & K_{2n} \\ K_{31} & K_{32} & K_{33} & \cdots & K_{3n} \\ \vdots & \vdots & \vdots & \ddots & \vdots \\ K_{n1} & K_{n2} & K_{n3} & \cdots & K_{nn} \end{pmatrix} \begin{Bmatrix} D_1 \\ D_2 \\ D_3 \\ \vdots \\ D_n \end{Bmatrix} = \begin{Bmatrix} F_1 \\ F_2 \\ F_3 \\ \vdots \\ F_n \end{Bmatrix} \text{ or } \mathbf{KD} = \mathbf{F}, \tag{1}$$

where **K** is the global stiffness matrix, **D** is the displacement variables vector, and **F** is the forcing vector. The global stiffness matrix is an $n \times n$ symmetric matrix. The diagonal entries K_{ii} represent the sum of contributing sub-matrices for the *i-th* block, such as strain energy, inertia, and body forces. The non-diagonal entries K_{ij} $(i \neq j)$ represent the sum of contributing sub-matrices of interaction between blocks i and j, such as contact forces. The total number of the displacement unknowns is the sum of the degrees of freedom of all the blocks. A complete description of the stiffness formulation matrix and load vector assembly is provided by Shi (1993).

The solution of the system of simultaneous equilibrium equations is constrained by inequalities associated with block kinematics: no penetration and no tension condition between blocks, which are imposed using the penalty method. Shear displacement along the interfaces is modeled using the Coulomb–Mohr failure criterion. The large displacements and deformations are the accumulation of small displacements and deformations at each time step.

The time integration scheme in DDA adopts the Newmark (1959) approach, which for a single degree of freedom can be written in the following manner:

$$\begin{aligned} u_{i+1} &= u_i + \Delta t \dot{u}_i + (0.5 - \beta)\Delta t^2 \ddot{u}_i + \beta \Delta t^2 \ddot{u}_{i+1} \\ \dot{u}_{i+1} &= \dot{u}_i + (1-\gamma)\Delta t \ddot{u}_i + \gamma \Delta t \ddot{u}_{i+1}, \end{aligned} \tag{2}$$

where $\ddot{u}$, $\dot{u}$, and u are acceleration, velocity, and displacement respectively, Δt is the time step, β and γ are the collocation parameters. Unconditional stability of the Newmark scheme is assured for $2\beta \geq \gamma \geq 0.5$. The DDA integration scheme uses $\beta = 0.5$ and $\gamma = 1$ and, thus it is implicit and unconditionally stable. The error propagated in the integration scheme may be attenuated or amplified depending on the collocation parameters used, however this discussion is beyond the scope of this contribution. For elaborate treatment of the subject, the reader is referred to Wang et al. (1996), who showed that $\beta = 0.5$ and $\gamma = 1$ assure highest attenuation rate (a.k.a algorithmic damping) and enhance solution convergence.

Computer implementation of DDA allows control over the analysis procedure through a set of user specified control parameters:

1. Dynamic control parameter ($k01$) – defines the type of analysis required, from quasi-static to fully dynamic. For quasi-static analysis the velocity of each block at the beginning of each time step is set to zero, $k01 = 0$. In case of dynamic analysis the velocity of each block at the end of a time step is fully transferred to the next time step, $k01 = 1$. Different values from 0 to 1 correspond to different degrees of inter step velocity transfer, comparable to damping or energy dissipation. For example, for an input value of $k01 = 0.95$ the velocity in the beginning of each time step is 5% lower than the terminal velocity at the previous time step.
2. Penalty value (p) – is the perpendicular stiffness of the contact springs used to enforce contact constrains between blocks. Tangential contact stiffness is assumed $p_t = 0.5p$.
3. Upper limit of time step size ($g1$) – the maximum time interval that can be used in a time step, should be chosen so that the assumption of infinitesimal displacement within the time step is satisfied.
4. Assumed maximum displacement ratio ($g2$) – the calculated maximum displacement within a time step is limited to an assumed maximum displacement ($U_{\max} = g2 \cdot (y/2)$, where y is the length of the analysis domain in the y-direction) in order to ensure infinitesimal displacements within a time step. This parameter is also used to detect possible contacts between blocks.

A necessary condition for direct input of dynamic acceleration is that the numerical computation has no artificial damping because artificial damping may lead to energy losses. In DDA the solution of the equilibrium equations is performed without damping.

4. Results of Validation Study

4.1 Analytical Model

For a block on an incline subjected to dynamic loading (Fig. 4) a Fourier series composed of sine components represents the simplest form of harmonic oscillations:

$$a(t) = \sum_{i=1}^{n} a_i \sin(\omega_i t), \tag{3}$$

where a_i and ω_i are the amplitude (acceleration) and frequency respectively.

The displacement of a mass subjected to dynamic loading is attained by double integration of the acceleration record (Eq. 2) from θ to t:

$$d(t) = \sum_{i=1}^{n} \frac{a_i}{\omega_i^2}[-\sin\omega_i t + \sin\omega_i\theta + \omega_i(t-\theta)\cos\omega_i\theta_i], \tag{4}$$

where θ is the time at which yield acceleration a_y is attained.

Hatzor and Feintuch (2001) showed that for an acceleration function consisting of sum of three sines (for arbitrary selected constants $a_1 = \omega_1 = 1$; $a_2 = \omega_2 = 2$; $a_3 = \omega_3 = 3$)

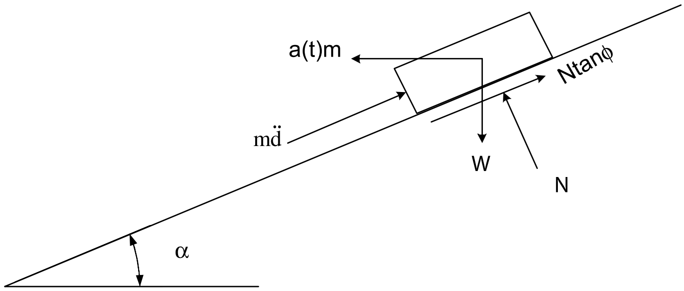

Fig. 4. Forces acting on a block on an incline subjected to dynamic loading (after Goodman and Seed, 1965)

DDA prediction is accurate within 15% of the analytic solution provided that the numeric control parameters g1, g2 are carefully selected. Moreover, they argued that the influence of higher order terms in a series of sines is negligible. These values produce a low frequency dynamic input assuring a nearly constant block velocity, which was attained at the beginning of the analysis (*ca*. 20% of elapsed time).

In order to attain a more realistic simulation we have extended the analysis to higher frequencies, constraining the peak horizontal acceleration to 0.15 g. The analysis was performed for a single block resting on a plane inclined $\alpha = 15°$ to the horizontal. The block material properties were: density $\rho = 2700\,\mathrm{kg/m^3}$, $\mathrm{E} = 5 \cdot 10^9\,\mathrm{N/m^2}$, and $v = 0.25$. The friction angle of the sliding plane was set to $\phi = 15°$, thus the yield acceleration ($a_y = 0$) was attained immediately at the beginning of analysis ($\theta = 0$ sec). Three different sets of frequencies were modeled (Table 2). Constant values of numeric spring stiffness ($p = 1 \cdot 10^9\,\mathrm{N/m}$), assumed maximum displacement ratio (g2 = 0.0075), and dynamic control parameter ($k01 = 1$) were used.

Input acceleration and comparison between the analytical solution and the numerical solution for the total displacements are presented in Fig. 5. The figure shows DDA solutions for two values of g1: 0.005 sec and 0.0025 sec, which yielded the most accurate results, larger time steps yielded lower accuracy.

The relative numeric error is defined by:

$$e(\%) = \frac{\|d - d_N\|}{\|d\|} \cdot 100, \tag{5}$$

and the relative numeric difference is defined by:

$$e'(\%) = \frac{\|d\| - \|d_N\|}{\|d\|} \cdot 100, \tag{6}$$

where d is the analytical or the measured displacement and d_N is the numeric displacement vectors respectively. $\|\cdot\|$ is the norm operator.

Table 2. Frequency sets for sum of three sines input function

Set	ω_1 (π), a_1 (g)	ω_2 (π), a_2 (g)	ω_3 (π), a_3 (g)
1	8, 0.1	4, 0.05	2, 0.025
2	10, 0.1	5, 0.05	2.5, 0.025
3	15, 0.1	7.5, 0.05	3.75, 0.025

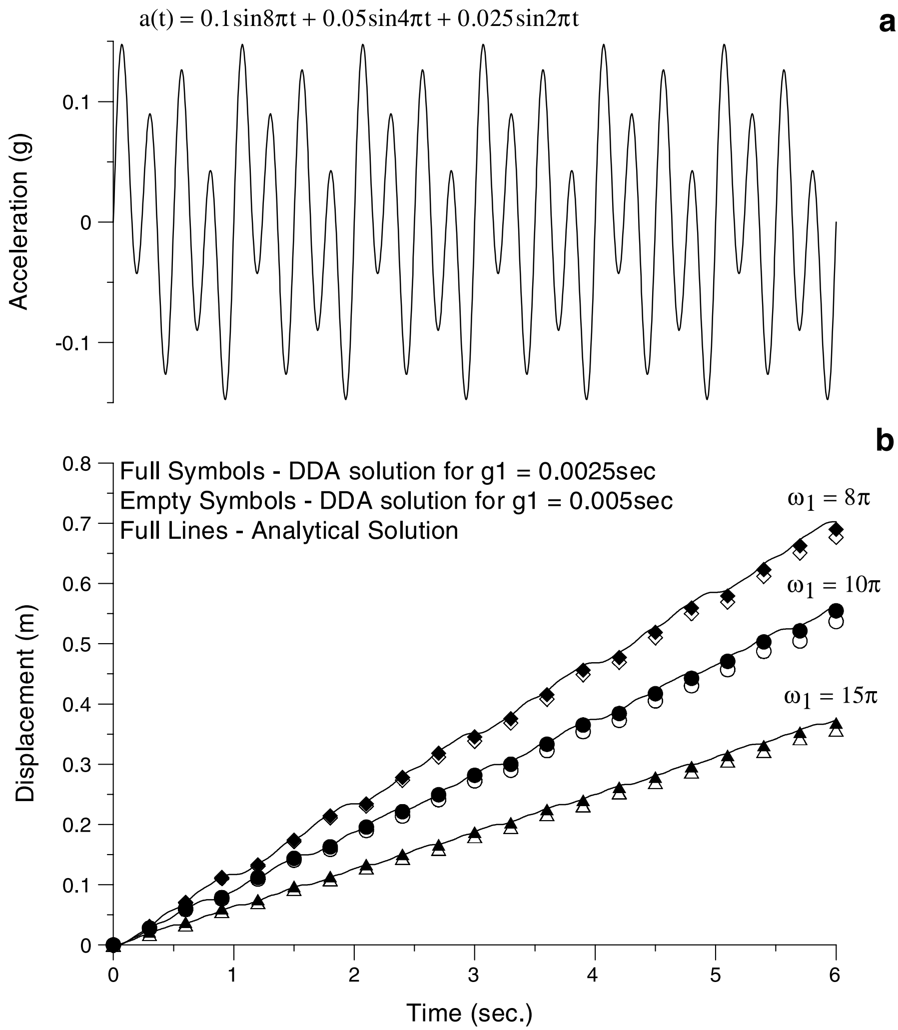

Fig. 5. a) The loading function $a(t) = a_1\sin(\omega_1 t) + a_2\sin(\omega_2 t) + a_3\sin(\omega_3 t)$; **b**) Comparison between analytical and DDA solution for block displacement subjected to a sum of three sines loading function. All DDA simulations for: $p = 1 \cdot 10^9\,\mathrm{N/m}$; g2 = 0.0075; block elastic modulus $E = 5 \cdot 10^9\,\mathrm{N/m^2}$. All input motions are $\omega_1 = 2\omega_2 = 4\omega_3$

The relative numeric error for g1 = 0.005 sec simulations is within 4.5% for a numeric spring stiffness of $p = 1 \times 10^9\,\mathrm{N/m}$. Halving the time step reduces the numeric error to 1.5%.

We have further investigated the interrelationship between the numeric control parameters using the input function of set 2 (Table 2). Figure 6 shows the dependence of the numeric error on the choice of the numeric control parameters g1, g2, and the numeric spring stiffness p. It is found that for an optimized set of g1 and g2 (bold in Fig. 6) the DDA solution is not sensitive to the penalty value, which can be changed over two orders of magnitude, from $p = 1 \times 10^8\,\mathrm{N/m}$ to $p = 5 \times 10^9\,\mathrm{N/m}$, with no

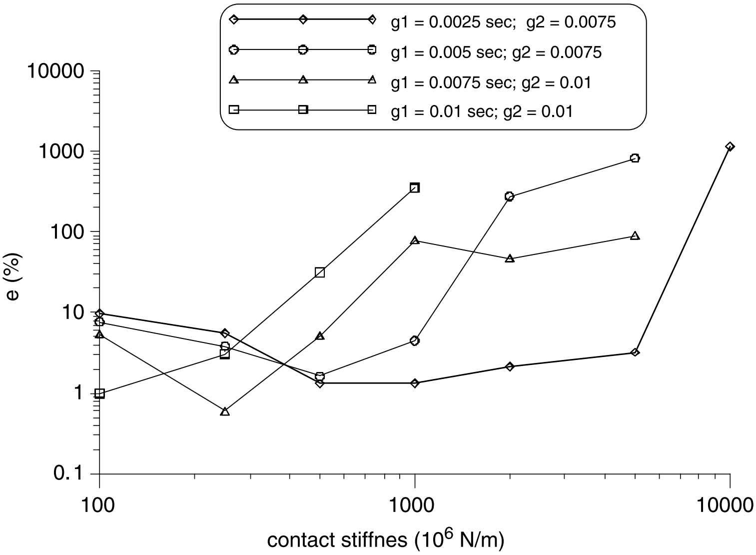

Fig. 6. Absolute numeric error of DDA ultimate displacement prediction as a function of spring stiffness, for a sum of three sines loading function

significant change in error. Within this range the numeric error never exceeds 10% and in most cases approaches the value of 1%. Departing from the optimal g1, g2 combination results in increased sensitivity of the DDA solution to the penalty value. The departure from the analytical solution occurs at lower penalty values with increasing time step size.

4.2 Shaking Table Experiments

It has been shown that there is a very good agreement between DDA and analytical solutions for the block on an incline problem. However, the analytical solution is only an approximation of the physical problem with various simplifying assumptions including: perfectly rigid block, constant friction, and complete energy conservation. Comparison between DDA and physical model results can help us probe into the significance of these assumptions.

For this part of the study the numeric control parameters are: penalty value $p = 5 \cdot 10^9\,\mathrm{N/m}$, time step size $\mathrm{g1} = 0.0025\,\mathrm{sec}$, assumed maximum displacement $\mathrm{g2} = 0.005$. Block elastic modulus is taken as $E = 200 \cdot 10^9\,\mathrm{N/m^2}$, which is the elastic modulus of steel. The 2.66 Hz input motion is discussed here in detail and the results are shown in Fig. 7. For $\mathrm{k01} = 1$ the numeric error is approximately 80%, but the ultimate displacement values are close, 0.055 m measured displacement compared to 0.093 m of calculated solution. Introducing some kinetic damping by reducing k01 improves the agreement between DDA and the physical test. Setting $\mathrm{k01} = 0.98$, corresponding to 2% velocity reduction, reduces the error to below 4%,

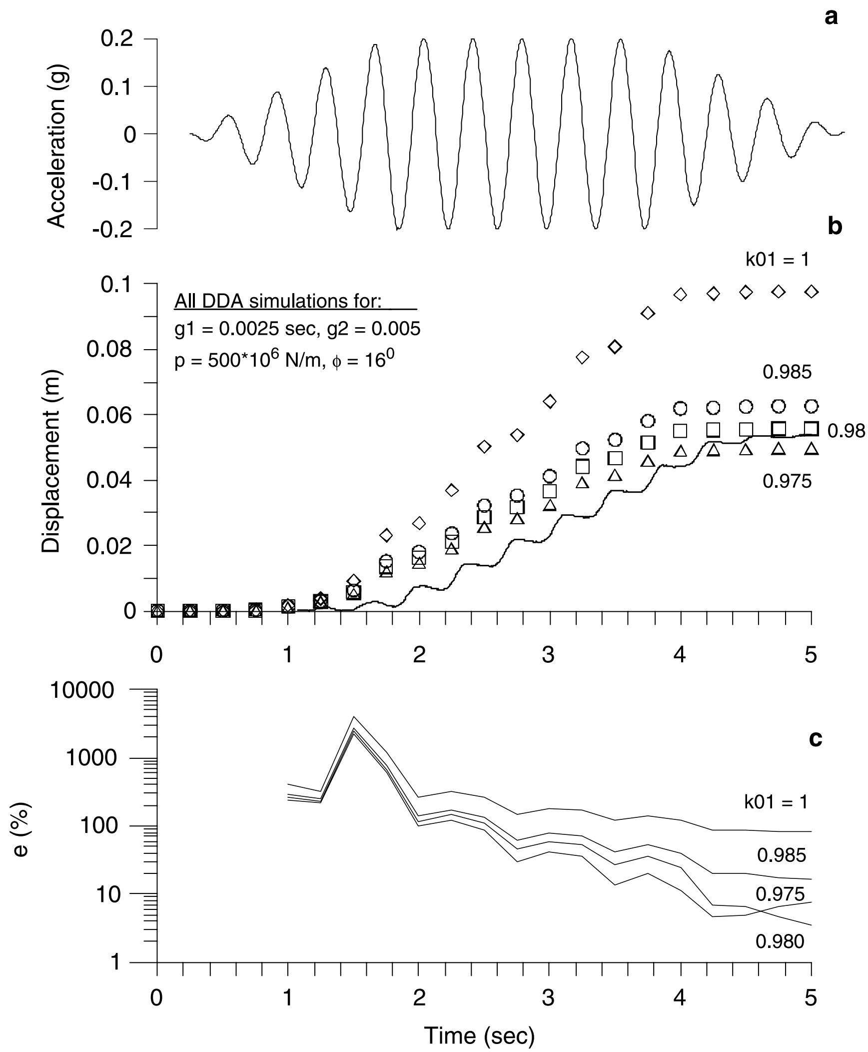

Fig. 7. a) The 2.66 Hz sinusoidal input function; **b**) Comparison of measured displacement and DDA solution for the 2.66 Hz test, for different values of dynamic control parameter (*k*01); **c**) Evolution of the numeric error during the test

and improves the tracking of the displacement history by DDA. Setting the k01 = 0.95 results in a highly un-conservative (underestimated) displacement prediction by DDA.

Plotting the relative numeric difference (e') against the input motion frequency (Fig. 7) shows that in general DDA accuracy increases with higher frequencies, and that for k01 = 1 the numeric error is always conservative (overprediction of displacement), with an exception at 6 Hz. Reducing k01 to 0.98 shows a similar effect for all frequencies, reducing the numeric error below 10%.

5. Discussion

The implicit formulation of DDA guarantees numerical stability regardless of time step size. However, it does not guaranty accuracy. Where the time step is too large relative to the numeric spring stiffness, loss of diagonal dominance and/or ill conditioning error may result, interfering with convergence to an accurate solution.

The numeric implementation of DDA utilizes the SOR Gauss–Seidel equation solver, the convergence of which is guarantied for diagonally dominant matrices. Larger inertia terms on the diagonal of the global stiffness matrix increase the stability of the computation. A small time step size is needed to increase the inertia terms, which are inversely proportional to the square of time step. For small time steps (0.0025 sec) the numeric error does not exceed $e = 10\%$ for increasing penalty values up to $5 * 10^{10}$ N/m; higher penalty values however result in significant error as the off diagonal sub-matrices become exceedingly large. Enlarging the time step results in reduction of inertia terms in the diagonal sub-matrices. Therefore, for a given time step size the loss of diagonal dominance will occur at lower penalty values.

Most of the error is accumulated at the beginning of the analysis and it declines with time, a phenomenon known as algorithmic damping, which is typical to the Newmark implicit time integration scheme (Fig. 7c). This behavior is observed here for all selected values of k01. In this study we have limited the duration of the analysis to 5 seconds, in conjunction with the duration of the shaking table experiment. Doolin and Sitar (2002) show that for a block on an incline problem the relative error continues to decrease up to displacement of 250 m during 16 seconds of sliding. Therefore, for computations involving larger time spans the error is expected to decline as calculation proceeds, further improving solution accuracy.

When compared with analytical solutions for frictional sliding DDA is found to be accurate. Therefore, it can be assumed that the contact formulation in DDA is

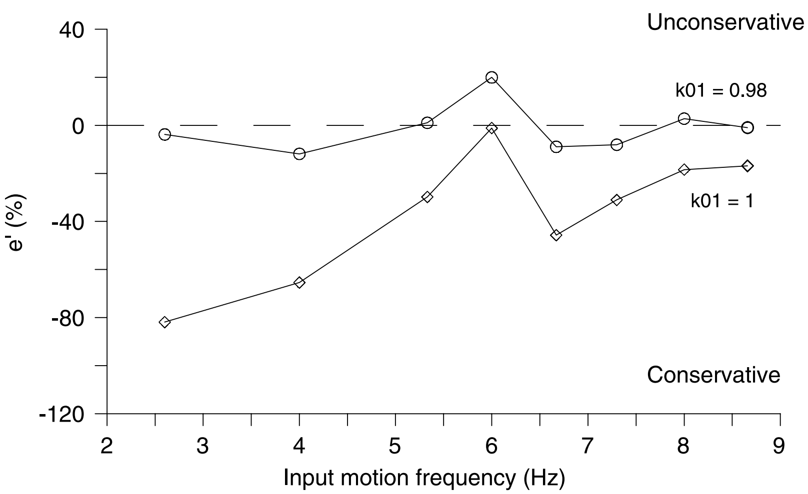

Fig. 8. Numeric error of DDA ultimate displacement prediction as a function of input frequency, for a sinusoidal input function

equivalent to the mathematical model for frictional sliding. The comparison with shaking table experiments however implies that the contact formulation in DDA is not sufficiently accurate for modeling physical friction. Consider for example the phenomenon of block "wobbling" during shaking table experiments. In the numerical model the acceleration is applied as a concentrated body force at the centroid of each block, whereas in the physical model block displacement is induced by the motion of the shaking table. This motion causes block "wobbling" during which physical contacts may open and close repeatedly. This process reduces the total energy of the system and consequently the total down-slope displacement. Furthermore, the dynamic formulation of DDA is essentially un-damped, friction being the main source of energy consumption. In the physical model however mechanisms such as structural vibrations, material damage along interface (ploughing), drag, heat etc. do take place during block sliding. These processes are not modeled numerically and can be a second source of discrepancy between the results of the numerical and physical models.

The only method available at present to simulate energy dissipation in DDA is by reducing transferred velocity between time steps. In this study it is found that a reduction of transferred velocity by 2% ($k01 = 0.98$) yields realistic prediction of block displacements, further reduction of the dynamic control parameter yields unconservatively small displacements.

The numeric analyses show good agreement with the shaking table results, once kinetic damping is applied. The reduction of the transferred velocity between timesteps is a numeric adaptation not linked directly to a physical damping mechanism. Since DDA formulation is essentially un-damped, viscous damping is not accounted for. Implementation of a dashpot model in parallel with a contact spring (Voigt model) in order to simulate viscous damping in DDA would be more appropriate. However, it is impossible to assign a correct damping coefficient for the given problem a priory. For problems of rock falls analyzed using DDA with viscous damping (Chen et al., 1996; Shingi et al., 1997) the selection of the damping coefficient was performed using trial and error procedure. We perform similar best "fitting" by reducing the transferred velocity between time steps.

The results reported herein are for a simple two block system. Natural slopes are more complex, containing many blocks of different geometries. When subjected to dynamic loading the blocks are expected to show different modes of failures resulting from blocks geometries and inter-block interactions. As shown in this research for a simple two block system a "kinetic damping" of 2% is required for accurate solution. It is expected that for a multi block system the amount of "kinetic damping" should be higher. McBride and Scheele (2001) showed that for a multi block array on a steep base under gravitational load the amount of required "kinetic damping" is about 20% ($k01 = 0.8$). However, this estimate should be examined in conjunction with conditioning of g1, g2 parameters. Hatzor et al. (2002), who studied the stability of a natural rock slope situated in seismically active zone using DDA, showed that most accurate results were obtained for "kinetic damping" lower than 5%. Higher values resulted in un-conservative slope behavior, while un-damped simulations resulted in excessive and non-realistic displacements.

6. Conclusions

1. The results of the validation study show that DDA solution of an idealized system for which an analytical solution exists, is accurate. The block contact algorithm in DDA is therefore an accurate replication of the analytical model for frictional sliding.

2. The accuracy of DDA is governed by the conditioning of the stiffness matrix. The DDA solution is accurate as long the chosen time step is small enough to assure diagonal dominance of the global stiffness matrix.

3. Comparison between shaking table experiments and DDA calculation shows that the DDA solution is generally conservative, over predicting block displacement. The main sources of discrepancy between DDA and the physical model are the difference between the numerical and actual behavior at contact points, and lack of a complex energy dissipation algorithm in DDA.

4. For accurate displacement prediction a reduction of the dynamic control parameter ($k01$) by 2% is recommended, for the block on a incline problem.

5. Implementation of viscous damping and strain/displacement dependent friction into DDA can further improve the accuracy of the method.

Acknowledgments

The writers acknowledge the financial support by the US – Israel Bi-national Science Foundation, trough Grant No. 98-399. The authors wish to express their gratitude to Gen-hua Shi who kindly provided his new dynamic version of DDA. Shaking table data were provided by J. Wartman of Drexel University, R. Seed, and J. Bray of University of California, Berkeley, and their cooperation is greatly appreciated.

References

Cai, Z., Bathurst, R. J. (1996): Deterministic sliding block methods for estimating seismic displacements of earth structures. Soil Dyn. Earthquake Eng. 15, 255–268.

Chen, G., Miki, S., Ohnishi, Y. (1996): Practical improvements to DDA. In: Reza Salami, M., Banks, M. (eds.). Proc., 1st International Forum on Discontinuous Deformation Analysis (DDA) and Simulation of Discontinuous Media. 97–110. Berkeley, 12–14 June. TSI Press, Albuquerque.

Crawford, A. M., Curran, J. H. (1981): The influence of shear velocity on the frictional resistance of rock discontinuities. Int. J. Rock Mech. Min. Sci. 18, 505–515.

Cundall, P. A. (1971): A computer model for simulating progressive, large scale movements in blocky rock system. Symposium of International Society of Rock Mechanics, Nancy, France, 11–18.

Doolin, D., Sitar, N. (2002): Displacement accuracy of discontinuous deformation analysis applied to sliding block. J. Engng. Mech. ASCE 128(11), 1158–1168.

Goodman, R. E., Seed, H. B. (1965): Earthquake induced displacements in sand embankments. J. Soil Mech. Foundations Div. ASCE 92(SM2), 125–146.

Hatzor, Y. H., Feintuch, A. (2001): The validity of dynamic block displacement prediction using DDA. Int. J. Rock Mech. Min. Sci. 38, 599–606.

Hatzor, Y. H., Arzi, A. A., Tsesarsky, M. (2002): Realistic dynamic analysis of jointed rock slopes using DDA. In: Hatzor, Y. H. (ed). Proc., 5th International Conference on Analysis of Discontinuous Deformation.

Jibson, R. W. (1993): Predicting earthquake induced landslide displacements using Newmark's sliding block analysis. Transport. Res. Rec. 1411, 9–17.

Jibson, R. W., Harp, E. L., Michael, J. A. (1998): A method for producing digital probabilistic seismic landslides hazard maps: an example from the Los Angeles, California area. USGS. Open File Report 98–113.

Kim, J., Bray, J. D., Reimer, M. F., Seed, R. B. (1999): Dynamic interface friction properties of geosyntetics. Unpublished report, Department of Civil Engineering, University of California at Berkeley.

MacLaughlin, M. (1997): Discontinuous deformation analysis of the kinematics of rock slopes. Ph.D. thesis, Department of Civil Engineering, University of California, Berkley.

McBride, A., Scheele, F. (2001): Investigation of discontinuous deformation analysis using physical laboratory models. In: Bicanic, N. (ed.), Proc. Fourth International Conference on Discontinuous Deformation Analysis, 73–82.

Newmark, N. M. (1959): A method of computation for structural dynamics. J. Eng. Mech. Div. ASCE. 85(EM3).

Newmark, N. M. (1965): Effects of earthquakes on dams and embankments. Geotecnique 15(2), 139–160.

O'Sullivan, C., Bray, J. D. (2001): A comparative evaluation of two approaches to discrete element modeling to particulate media. In: Bicanic, N. (ed.), Proc., Fourth International Conference on Discontinuous Deformation Analysis. Glasgow, 6–8 June, 97–110.

Shi, G-H. (1988): Discontinuous deformation analysis – a new model for the statics and dynamics of block systems. Ph.D. thesis, Department of Civil Engineering, University of California, Berkley.

Shi, G-H. (1993): Block system modeling by discontinuous deformation analysis. In: Brebbia, C. A., Connor, J. J. (eds.), Topics in engineering, Vol. 11. Computational Mechanics Publication.

Shi, G-H. (1999): Applications of discontinuous deformation analysis and manifold method. In: Amadei, B. (ed.), Third International Conference on Analysis of Discontinuous Deformation, Vail, Colorado, 3–4 June, 3–16.

Shingi, M., Ohno, H., Otsuka, Y., Ma, G. (1997): Viscosity coefficient of the rock fall simulation. In: Ohnishi, Y. (ed.), Second International Conference on Analysis of Discontinuous Deformation. Kyoto, Japan, 10–12 June, 201–210.

Tsesarsky, M., Hatzor, Y. H., Sitar, N. (2002): Dynamic block displacement prediction – validation of DDA using analytical solutions and shaking table experiments. In: Hatzor, Y. H. (ed.), Proc., 5th International Conference on Analysis of Discontinuous Deformation, 195–206.

Wang, C.-Y., Chuang, C.-C., Sheng, J. (1996): Time integration theories for the DDA method with Finite Element meshes. In: Reza Salami, M., Banks, M. (eds.), Proc., Fifth nternational Forum on Discontinuous Deformation Analysis (DDA) and Simulation of Discontinuous Media. Berkeley, 12–14 June. TSI Press, Albuquerque, 97–110.

Wartman, J., Bray, J. D., Seed, R. B. (2003): Inclined plane studies of the Newmark sliding block procedure. Simplifying assumptions. J. Geotech. Geoenvironm. Engng. ASCE 129(8), 673–684.

Wilson, R. C., Keefer, D. K. (1983): Dynamic analysis of slope failure from the 6 August 1979 Coyote Lake, California earthquake. Bull. Seismol. Soc. Am. 73, 863–877.

Yeung, M. R. (1991): Application of Shi's DDA to the study of rock behavior. Ph.D. thesis, Department of Civil Engineering, University of California, Berkley.

Author's address: Dr. Michael Tsesarsky, Postdoctoral Fellow, Faculty of Civil Engineering, Technion, 32000 Haifa, Israel; e-mail: michaelt@technion.ac.il